Revista Brasileira de Ciências Ambientais
Brazilian Journal of Environmental Sciences

Climatic regionalization of the Brazilian Semi-Arid Region and its sociodemographic dynamics

Zoneamento climático no Semiárido do Brasil e sua dinâmica sociodemográfica

Renata Barbosa Monteiro Machado[1], *Flávia Ferreira Batista*[1], *Lara de Melo Barbosa Andrade*[1], *Albert Smith Feitosa Suassuna Martins*[1], *Cláudio Moisés Santos e Silva*[1]

ABSTRACT

The history of the Brazilian Semi-Arid (BSA) region is intrinsically linked to extreme climatic variations, such as prolonged droughts and increasing aridity, which severely impact water security, food security, and socioeconomic stability in the region. The aim of this study was to develop a homoclimatic typology for the BSA by identifying homogeneous climatic profiles and associating them with sociodemographic dynamics. Meteorological data, including precipitation, relative humidity, maximum and minimum temperatures, and wind speed, were obtained from the Brazilian Daily Weather Gridded Data, interpolated on a 0.1 × 0.1° grid, covering the period from 1961 to 2020. Additionally, 18 sociodemographic indicators from the 1991, 2000, and 2010 censuses, carried out by the Brazilian Institute of Geography and Statistics, such as infant mortality and urbanization rates, were analyzed. Through cluster analysis using the Ward method, four distinct climatic zones (BSA I, II, III, and IV) were identified. This approach enabled the integration of meteorological and sociodemographic variables, providing a more precise characterization of the region. The results revealed rising temperatures, intensifying droughts, and increased vulnerability in areas such as BSA III, characterized by severe aridity and limited infrastructure. Despite improvements in sociodemographic indicators, regional inequalities persist, underscoring the importance of examining age and sociodemographic characteristics within the identified clusters. This analysis aims to understand the population-specific characteristics of each profile and their relationship with existing vulnerabilities, enabling the identification of specific patterns and supporting the formulation of more targeted and effective public policies.

Keywords: cluster analysis; population censuses; homogeneous regions; climatic regionalization.

RESUMO

A história do Semiárido Brasileiro está intrinsecamente ligada a variações climáticas extremas, como secas prolongadas e aumento da aridez, que impactam severamente a segurança hídrica, alimentar e socioeconômica da região. Este estudo buscou desenvolver uma tipologia homoclimática para o SAB, identificando perfis climáticos homogêneos e associando-os à dinâmica sociodemográfica. Foram utilizados dados meteorológicos, como precipitação, umidade relativa do ar, temperaturas máximas e mínimas e velocidade do vento, obtidos do banco de dados *Brazilian Daily Weather Gridded Data*, interpolados em uma grade de 0,1 × 0,1°, cobrindo o período de 1961 a 2020. Ademais, foram analisados 18 indicadores sociodemográficos dos Censos de 1991, 2000 e 2010, realizados pelo Instituto Brasileiro de Geografia e Estatística, como mortalidade infantil e urbanização. Por meio da análise de agrupamentos (*cluster analysis*) utilizando o método de *Ward*, foram identificadas quatro zonas climáticas distintas (SAB I, II, III e IV). Tal abordagem permitiu integrar variáveis meteorológicas e sociodemográficas, oferecendo uma caracterização mais precisa da região. Os resultados revelaram aumento de temperaturas, intensificação de secas e maior vulnerabilidade em áreas como o SAB III, marcado por aridez severa e infraestrutura limitada. Apesar de avanços nos indicadores sociodemográficos, as desigualdades regionais persistem e, com isso, evidenciam a necessidade de analisar os indicadores etários e sociodemográficos nos *clusters* identificados, com o intuito de compreender as particularidades populacionais de cada perfil e sua relação com as vulnerabilidades existentes, permitindo identificar padrões específicos, como também subsidiar a formulação de políticas públicas mais direcionadas e eficazes.

Palavras-chave: análise de *clusters*; censos populacionais; regiões homogêneas; regionalização climática.

[1] Federal University of Rio Grande do Norte – Natal (RN), Brazil.
Corresponding author: Renata Barbosa Monteiro Machado – Centro de Ciências Exatas e da Terra, Programa de Pós-Graduação em Ciências Climáticas – Campus Universitário Lagoa Nova – CEP: 59078-970 – Natal (RN), Brazil. E-mail: renata.monteiro.639@ufrn.edu.br
Conflicts of interest: the authors declare no conflicts of interest.
Funding: This research was supported by the Coordination for the Improvement of Higher Education Personnel (CAPES), Brazil, under Finance Code 001.
Received on: 06/16/2025. Accepted on: 11/19/2025.
https://doi.org/10.5327/Z2176-94782654

This is an open access article distributed under the terms of the Creative Commons license.

Introduction

The impacts of climate change, including the increased frequency of extreme events, tend to be more severe in tropical countries such as Brazil due to a combination of environmental, social, and economic vulnerabilities, which can result in significant consequences such as biodiversity loss and worsening social inequalities (Nobre et al., 2016; Rathore, 2024). Global warming, characterized by an increase in the Earth's average temperature, has altered rainfall patterns in the Brazilian Semi-Arid (BSA) region, intensifying droughts and increasing water and food insecurity, especially in communities with low adaptive capacity (Barbosa, 2024; Guedes et al., 2024).

In the global context, climate change amplifies rainfall variability and the occurrence of prolonged droughts, especially in arid and semi-arid zones, where studies such as those by Huang et al. (2016), Sanzheev et al. (2020), Ullah et al. (2021), and Yao et al. (2021) highlight that the increase in average temperature and changes in precipitation patterns intensify environmental degradation, which can directly affect vulnerable populations. Recent studies confirm, for example, that regions of the African Sahel, Northeast China, Western North America, and South America, in areas of Argentine Patagonia, the Andes, and Northeast Brazil (NEB), have already experienced significant reductions in precipitation and increases in evapotranspiration, which has intensified the accelerated process of aridification (Scholes, 2020; Vaidyanathan et al., 2020; Alvar-Beltrán et al., 2021; Blanco and Doyle, 2024; Dzvene et al., 2025).

The Intergovernmental Panel on Climate Change (IPCC) highlights that semi-arid regions, such as the BSA, are among the most sensitive to climate change, with projections of increased aridity, risk of desertification, and water insecurity (Burrell et al., 2020; Huang et al., 2020; IPCC, 2023). Studies indicate an increase in the frequency and severity of droughts, impacting water availability and the socioeconomic sustainability of the region (Reis et al., 2020; Santos et al., 2022; Santos et al., 2024). Global warming and changes in atmospheric circulation have amplified these extreme events (Medeiros et al., 2020; Reis et al., 2020; Brito et al., 2022; Espinoza et al., 2024; Marengo, 2024).

The BSA also faces historical and structural challenges, marked by low human development indices and high levels of social exclusion. These factors, combined with climate pressures, perpetuate poverty and limit development opportunities (Ribeiro et al., 2022; Guedes et al., 2024). Between 2012 and 2017, the region faced one of the longest droughts in its history, with a sharp drop in rainfall and expansion of unproductive areas (Santana and Santos, 2020). Desertification, aggravated by inappropriate land use practices, threatens biodiversity and ecosystem resilience (Tomasella et al., 2018; Paredes-Trejo et al., 2023).

The intensification of climate change requires adaptation and mitigation strategies, and the zoning of vulnerable areas is an important tool for identifying regions at risk and implementing sustainable solutions, as shown in studies by Tinôco et al. (2018), Albuquerque et al. (2020), Mutti et al. (2020), and Silveira et al. (2020), who used statistical analyses to classify climate regions and identify agricultural and socioeconomic vulnerabilities.

Unlike previous studies, which addressed the creation of homoclimatic profiles of the BSA based on a single meteorological variable (Oliveira et al., 2016; Tinôco et al., 2018; Abreu et al., 2019; Alves et al., 2021; Zabalaga et al., 2022), this research integrates five meteorological variables applied specifically to the BSA context, using cluster analysis to characterize its climatic specificities, with the differential of integrating these climatic characteristics with social and demographic data from three Demographic Censuses, which enabled the construction of a climatic typology that more accurately reflects the particularities of the BSA. This approach provides a more robust basis for the development of policies and strategies aimed at the sustainable management of natural resources and strengthening the resilience of the local population to the impacts of climate change (Marengo et al., 2017).

In this context, the objective of this study is to establish a homoclimatic typology in the BSA, combining meteorological variables with sociodemographic indicators in order to identify homogeneous climate zones and their relationship with population dynamics, using cluster analysis to identify patterns of vulnerability and support more targeted public policies.

Materials and Methods

Study area

The BSA covers nine states in the Northeast: Alagoas, Bahia, Ceará, Maranhão, Paraíba, Pernambuco, Piauí, Rio Grande do Norte, and Sergipe, as well as some municipalities in Minas Gerais and Espírito Santo, in the Southeast Region (Figure 1), with a territorial area of approximately 1,182,697 km², comprising a total of 1,427 municipalities and corresponding to 15.5% of the Brazilian national territory (Sudene, 2021).

The BSA has an average annual rainfall of 800 mm, higher than other semi-arid regions, but is characterized by marked temporal and spatial variability. In the North, rainfall is concentrated between March and May, with up to 310 mm, while in the South it occurs from December to February, with up to 389 mm (Marengo, 2020; Silva et al., 2023). This variability requires water management and agricultural planning strategies, given the climate vulnerability. Average temperatures range from 24 to 27°C, with precipitation concentrated in 3 to 4 months, resulting in a negative water balance and high aridity index (Souza et al., 2015; Mutti et al., 2020; Vieira et al., 2021).

Data

The meteorological variables used include precipitation (mm), relative humidity (%), maximum and minimum temperatures (°C), and wind speed (m/s), data obtained from the Brazilian Daily Weather Gridded Data (BR-DWGD) database, developed by Xavier et al.

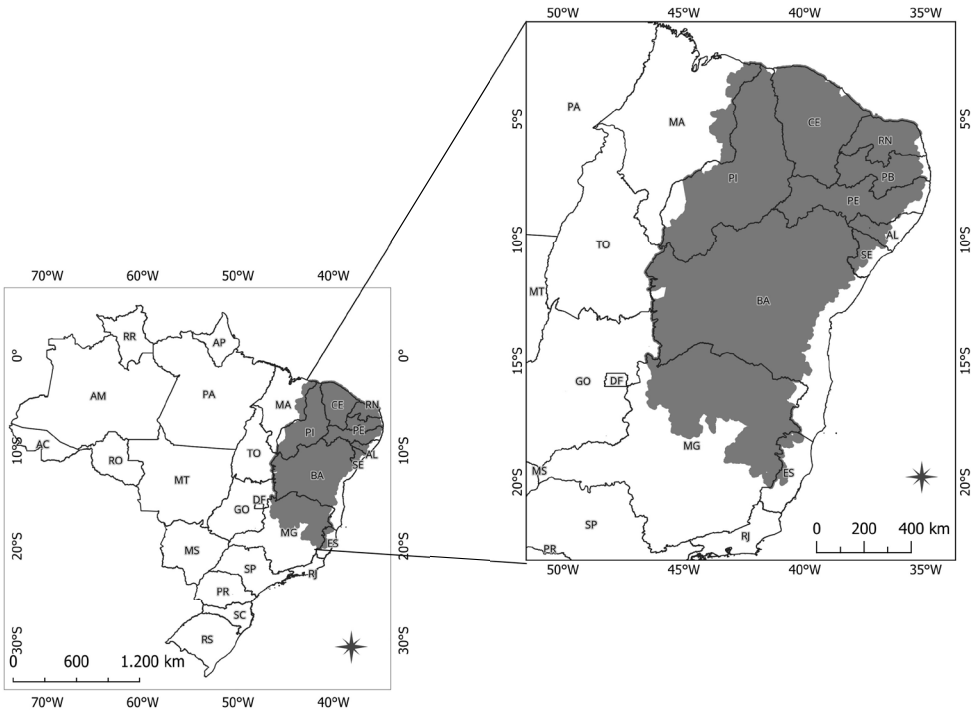

Figure 1 – Delimitation of the Semi-Arid region of Brazil

(2022), in collaboration between the University of Texas and the Federal University of Espírito Santo.

The BR-DWGD presents daily data in a regular grid with a spatial resolution of 0.1 × 0.1°, allowing for detailed representation of the spatial and temporal variability of meteorological variables. The dataset integrates information from 11,473 rain gauges and 1,253 weather stations, in addition to grid-interpolated topographic data. The coverage period ranges from January 1, 1961, to July 31, 2020, except for the precipitation variable, whose time series extends until December 31, 2022. The database is publicly accessible and available on the authors' website (Xavier et al., 2022).

Demographic and socioeconomic indicators

The demographic and socioeconomic analysis is based on data from the 1991, 2000, and 2010 Demographic Censuses (IBGE, 1991; 2000; 2010). Notably, 18 indicators were selected to characterize living conditions and human development in the BSA, organized into four dimensions:

- Population: total population, proportion of men and women, dependency ratio, aging index, life expectancy at birth, fertility rate, and infant and under-five mortality rates. These indicators provide an understanding of the age structure and patterns of reproduction and mortality.
- Education: illiteracy rate among the population aged 15 and over, which is essential for assessing human capital and educational inequalities.
- Income: proportion of individuals living in poverty and Municipal Human Development Index (MHDI), representative of local economic conditions.
- Households: access to piped water, sewage, garbage collection, electricity, and percentage of urbanization, reflecting basic infrastructure and quality of life. The selection of these indicators provides insights into socioeconomic inequalities and structural challenges in the region, considering areas with homogeneous meteorological characteristics.

This approach allows for the investigation of social and demographic transformations, integrating climatic effects into regional development. In addition, it contributes to the understanding of vulnerability and resilience in the BSA by integrating socioeconomic conditions with climate typology (Silva et al., 2023).

Statistical analysis and procedures

To identify homogeneous structures and underlying relationships in the BSA region, hierarchical cluster analysis was applied, using monthly and annual averages of climatological variables from the BR-DWGD dataset (Xavier et al., 2022). This method is widely used for

climate regionalization and enables more accurate climate monitoring and forecasting (Mingoti, 2013; Tinôco et al., 2018).

The methodological procedure comprised three main steps: i. selection of the similarity measure and linkage method; ii. application of the clustering algorithm; and iii. determination of the number of homogeneous groups (Lattin et al., 2011). For the first step, Euclidean distance was adopted as a measure of dissimilarity. Equation 1 describes its calculation, where xi,k and xj,k are the k variables of points i and j, respectively, and p corresponds to the total number of variables analyzed.

$$d_e = |x_i - x_j| = \left[\sum_{k-1}^{p} (x_{i,k} - x_{j,k})^2\right]^{0,5} \quad (1)$$

The Ward method (1963) was selected for clustering, as it minimizes intra-group variance and maximizes heterogeneity between clusters, resulting in homogeneous and well-balanced groups (Everitt and Dunn, 2010).

The determination of the optimal number of clusters was based on a combined assessment of quantitative and visual criteria. The dendrogram, which graphically represents the distances between observations and the hierarchical linkage among groups, was examined to define the cutoff point at which the branches exhibited the greatest dissimilarities, ensuring the formation of cohesive and distinct clusters (Hair et al., 2009; Everitt et al., 2011). In addition, the cophenetic correlation coefficient (CCC) was calculated to evaluate the degree of correspondence between the original distance matrix and the dendrogram-derived distances. Values close to 1 indicate a faithful representation of the underlying data structure. Values close to 1 indicate an accurate representation of the data structure (Everitt et al., 2011). All clustering analyses were performed using R software (version 4.3; Team, 2023), with the cluster and factoextra packages.

Following the definition of the climate clusters, a descriptive analysis of the meteorological variables and sociodemographic indicators for the three census periods (1991, 2000, and 2010) was performed. Next, the Kruskal–Wallis test was applied to each variable to verify whether the sociodemographic conditions differed significantly between the identified climate regions. This nonparametric test compares the distributions of medians between groups and is used to assess whether the observed differences are statistically significant (Wilks, 2011).

In the context of this study, the null hypothesis assumes that all regions (clusters) belong to the same population, that is, that there are no significant differences in sociodemographic variables between clusters. The alternative hypothesis indicates that at least one region exhibits behavior distinct from the others. A significance level of 5% (α=0.05) was adopted for the statistical decision-making. All statistical procedures were conducted in the R environment (R Core Team, 2023).

Results

The results obtained aimed to characterize the climatic variability of the BSA between 1961 and 2019 through an integrated analysis of meteorological parameters and sociodemographic indicators and revealed distinct spatial patterns of climatic homogeneity. The analysis of homogeneous clusters (BSA I to IV) showed significant variations in precipitation, temperature, air humidity, and wind speed, allowing the identification of regions with similar climatic behavior and their direct implications for population dynamics, agriculture, and regional development. Compared with previous studies that analyzed variables in isolation, this multivariate approach constitutes a methodological improvement and provides more robust support for planning adaptive actions in response to climate change in the region.

Spatial distribution of BSA meteorological variables (1961 to 2019)

The BSA is characterized by scarce and irregular rainfall, with high interannual variability. Average precipitation ranges from 200 mm to 800 mm and may be higher in specific areas. Between 1961 and 2019, the mean annual precipitation was 838.53 mm. The precipitation map illustrates the spatial distribution of rainfall across the region, based on a color scale ranging from blue to red (Figure 2).

The light blue areas (Figure 2A) indicate higher rainfall volumes (ranging from 1,000 to 1,200 mm yr^{-1}), while shades of red represent lower rainfall (below 400 mm yr^{-1}). Higher precipitation is concentrated in coastal zones and areas of higher elevation, whereas orange and red tones in the central portion of the region indicate lower rainfall totals. Municipalities with annual averages below 500 mm are mainly located in the central BSA, particularly in Bahia, Pernambuco, and parts of Paraíba. Macururé (BA) recorded the lowest mean annual precipitation (406.81 mm), whereas Mata Grande (AL) presented the highest value (1,720.48 mm).

The mean annual maximum air temperature in the BSA ranges from 25 to 35°C and may exceed 36°C in central and semi-arid areas (Figure 2B). Coastal zones and regions at higher elevations, represented by bluish tones, exhibit more moderate temperatures, ranging between 27.5 and 30°C. A clear thermal gradient is observed, with higher temperatures in the central portion of the region and lower temperatures along the coast and in elevated areas, influenced primarily by altitude, proximity to the ocean, and regional climatic conditions. Municipalities with mean maximum temperatures above 33°C are concentrated in Piauí, Rio Grande do Norte, Ceará, and Paraíba. Piatã (BA) showed the lowest average (25.25°C), while Paes Landim (PI) showed the highest (34.03°C).

The mean annual minimum air temperature varies between 14 and 24°C (Figure 2C), with the lowest value recorded in Itacambira (MG) (14.32°C) and the highest in Caucaia (CE) (23.59°C). Elevated areas, such as the Chapada Diamantina (BA), present minimum temperatures below 16°C, whereas low-altitude regions in the central and northern BSA exhibit mean values above 22°C. This spatial pattern reflects the influence of factors such as altitude and latitude, with direct implications for agricultural activities and thermal comfort.

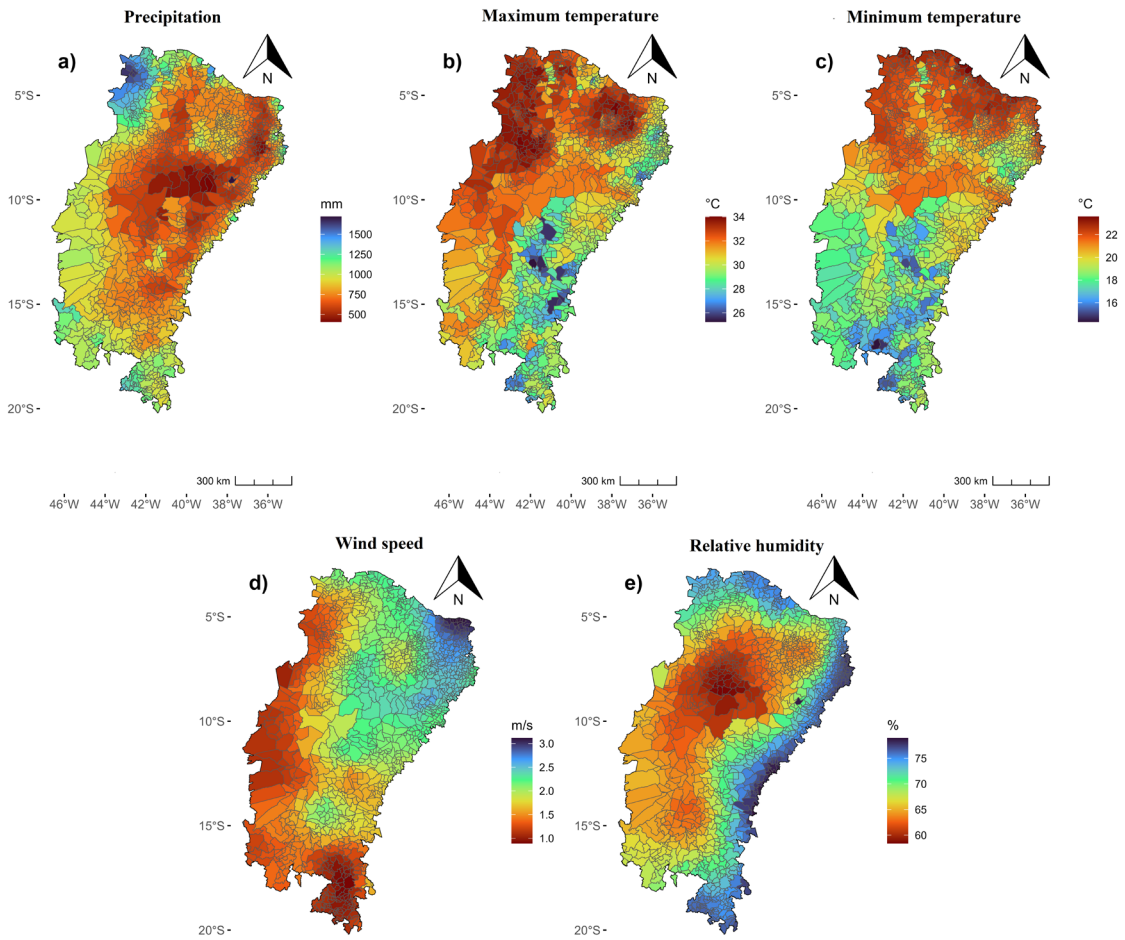

Figure 2 – Spatial distribution of annual averages for precipitation, maximum and minimum temperatures, relative humidity, and wind speed in the BSA (1961–2019).

The mean annual wind speed ranges from 3 m s^{-1} to 6 m s^{-1} and may exceed 10 m s^{-1} in exposed areas (Figure 2D). The lowest value was recorded in Teófilo Otoni (MG) (0.89 m s^{-1}), while the highest occurred in São Bento do Norte (RN) (3.12 m s^{-1}). Higher wind speeds are observed along the coastline and in specific inland areas, influencing wind energy potential, environmental planning, and climate-related studies.

Relative air humidity in the BSA ranges from 58% to 80% (Figure 2E), with the lowest mean value observed in Lagoa do Barro do Piauí (PI) (58.40%) and the highest in Cabaceiras do Paraguaçu (BA) (78.95%). Coastal areas and regions near watercourses generally exhibit humidity levels above 70%, whereas semi-arid zones tend to present values below 50%, directly affecting agricultural practices and water resource management.

Descriptive and spatial analysis of clusters

Figures 3A and 3B present the results of the hierarchical cluster analysis of climatic variables in the BSA region. The study identified four homogeneous climatic clusters in the BSA based on precipitation, temperature, relative humidity, and wind speed, using Ward's method to reduce seasonal variability (Moura et al., 2019). The temporal analysis (1961–2019) resulted in the construction of a hierarchical dendrogram that enabled the organization of regional climatic patterns (Hair et al., 2009). The optimal number of groups (k=4) was confirmed by the mean silhouette width (Figure 6B). The quality of the clustering was assessed using the CCC, which showed higher consistency for relative air humidity (CCC=0.743) and greater variability for precipitation (CCC=0.614), resulting in an overall CCC of 0.618. These results demonstrate that the adopted methodology effectively captured the spatial and temporal variability of the regional climate, ensuring internal homogeneity among the identified clusters.

Figure 4 analyzes three distinct periods: (A) 1961 to 2019; (B) 1961 to 1990; and (C) 1991 to 2019, aimed at assessing temporal changes in key climatic conditions, such as temperature and precipitation. The clusters, which represent distinct homoclimatic profiles, were desig-

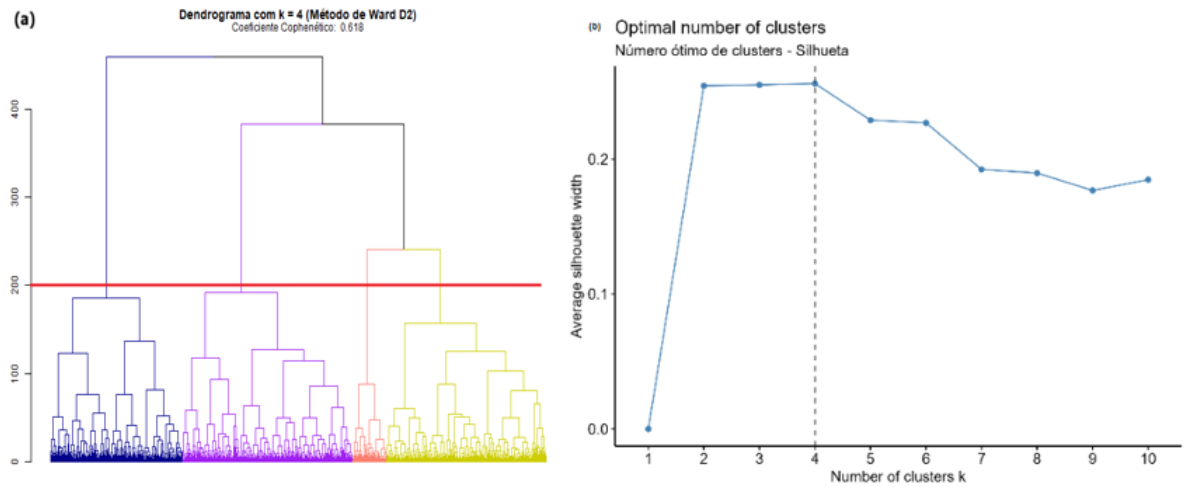

Figure 3 – Formation and validation of climate clusters. (A) Hierarchical dendrogram with a cutoff defining four clusters; (B) average silhouette width used to indicate the optimal number of clusters.

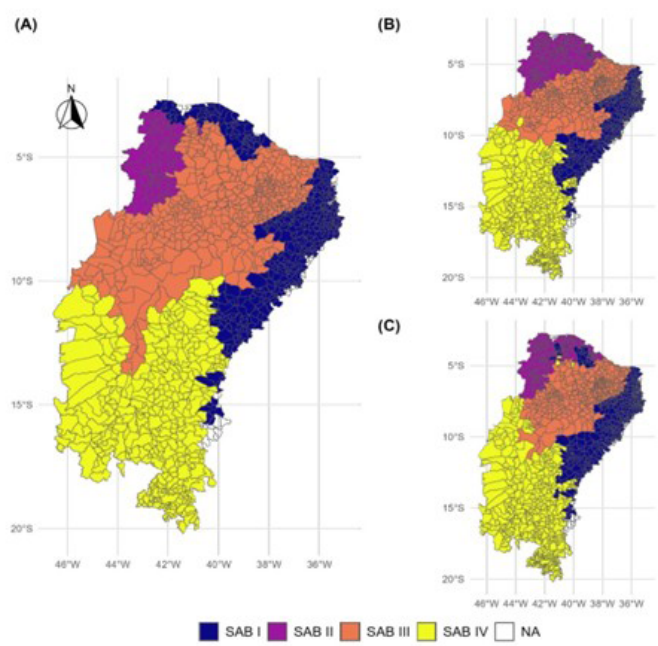

Figure 4 – Spatial classification of municipalities in the Brazilian Semi-Arid region into climate clusters based on climatological variables across different time periods. (A) Period: 1961–2019, (B) period: 1961–1990, (C) period: 1991–2019.

nated BSA I, BSA II, BSA III, and BSA IV. The analysis emphasizes the pronounced climatic diversity of the BSA region, highlighting the role of topography, particularly altitude, and atmospheric dynamics in shaping local and regional climatic conditions.

Table 1 presents the descriptive statistics of the main meteorological variables for the climate clusters BSA I, BSA II, BSA III, and BSA IV over the period from 1961 to 2019. The table summarizes mean values, standard deviations, and minimum and maximum records for the analyzed variables, including precipitation, maximum and minimum temperatures, relative humidity, and wind speed, thereby highlighting the climatic contrasts among the identified clusters.

The BSA comprises 1,427 municipalities, unevenly distributed among the climate clusters. BSA I includes 491 municipalities (34.41%), followed by BSA III with 459 municipalities (32.17%). BSA IV encompasses 379 municipalities (26.56%), while BSA II represents the smallest share, with 98 municipalities (6.87%). These spatial differences reflect the influence of local environmental factors, such as vegetation cover, altitude, and topographic features, on regional climate patterns.

Figure 4A illustrates the spatial distribution of the four homogeneous climate clusters in the BSA for the period 1961–2019. BSA I, covering areas along the eastern and northeastern coast, reflects the strong influence of coastal processes on regional climatic segmentation. This cluster records an average annual precipitation of 788.33 mm, with mean maximum and minimum temperatures of 30.0°C and 20.46°C, respectively. BSA I also exhibits the highest relative humidity (74.05%) and an average wind speed of 2.36 m/s (Table 1).

BSA II, located in the northwestern portion of the region (Figure 4A), presents the highest average annual precipitation (1,300.73 mm) and elevated maximum temperatures (33.44°C), along with a relative humidity of 69.11%. BSA III, situated in the north-central sector, shows the lowest precipitation values (753.64 mm), greater climatic variability, lower relative humidity (64.74%), and stronger winds (2.10 m/s). BSA IV, encompassing southern Bahia and northern

Table 1 – Descriptive statistics of meteorological variables in climate clusters BSA I, BSA II, BSA III, and BSA IV (1961–2019).

Precipitation (mm)				
Cluster	Mean value	SD value	Min value	Max value
BSA I	788.33	337.10	64.05	3179.26
BSA II	1300.73	406.08	414.87	3326.65
BSA III	753.64	297.46	73.80	3033.59
BSA IV	886.85	307.60	146.55	2671.94
Maximum temperature (°C)				
Cluster	Mean value	SD value	Min value	Max value
BSA I	30.00	1.49	23.43	35.18
BSA II	33.44	1.04	29.41	36.11
BSA III	32.48	1.33	26.84	36.52
BSA IV	29.14	1.76	22.17	34.98
Minimum temperature (°C)				
Cluster	Mean value	SD value	Min value	Max value
BSA I	20.46	1.50	14.05	24.82
BSA II	22.03	0.64	19.05	24.47
BSA III	21.15	1.25	15.20	24.79
BSA IV	17.64	1.32	12.77	21.79
Relative humidity (%)				
Cluster	Mean value	SD value	Min value	Max value
BSA I	74.05	4.28	52.85	85.55
BSA II	69.11	4.85	51.15	80.16
BSA III	64.74	5.28	46.04	80.11
BSA IV	70.47	5.73	52.17	86.01
Wind speed (m/s)				
Cluster	Mean value	SD value	Min value	Max value
BSA I	2.36	0.48	0.75	4.46
BSA II	1.50	0.45	0.39	4.41
BSA III	2.10	0.54	0.39	4.15
BSA IV	1.46	0.47	0.19	3.44

Minas Gerais, records the second highest precipitation (886.85 mm), the mildest thermal conditions (29.14°C maximum and 17.64°C minimum), and the lowest average wind speed (1.46 m/s) (Table 1).

A comparison between the periods 1961–1990 (Figure 4B) and 1991–2019 (Figure 4C) reveals shifts in the boundaries of the climate clusters. BSA I, characterized by lower precipitation and higher temperatures, expanded inland, currently covering 34.41% of the Semi-Arid region and 491 municipalities, whereas BSA II, previously more humid, experienced a contraction, accompanied by reduced precipitation and higher temperatures. These changes may be associated with climatic variability, atmospheric circulation patterns, topographic influences, and land-use changes. In the most recent period (1991–2019), a possible expansion of BSA IV was observed, alongside increasing mean temperatures, declining precipitation, and the expansion of arid areas across the Semi-Arid region. Furthermore, prolonged drought events have intensified water losses, exacerbating regional climate challenges (Barbosa, 2023; IPCC, 2023).

Analysis of demographic dynamics and socioeconomic indicators

The analysis of population dynamics between 1991 and 2010, in relation to the climatic characteristics of the clusters, highlights the combined influence of environmental and socioeconomic factors on demographic change. BSA I exhibited steady population growth (from 38.76 to 39.50%), driven by moderate climatic conditions and diversified economic activities. BSA II, characterized by a humid and warm climate, recorded the highest growth rate (24.9%, increasing from 7.71 to 8.20%), largely supported by agricultural expansion. BSA III experienced moderate growth (from 27.92 to 28.53%), despite arid conditions, indicating a degree of regional resilience. In contrast, BSA IV showed the lowest growth rate (9.1%) and a decline in its share of the total population (from 25.61 to 23.77%), suggesting that socioeconomic constraints, such as limited employment opportunities and infrastructure, strongly influence migration patterns.

Between 1991 and 2010, BSA II presented the highest annual population growth rates (1.17 and 1.08%), driven by migration flows and socioeconomic development. BSA I and BSA III maintained relatively stable growth trajectories, while BSA IV recorded the lowest rates (declining from 0.50 to 0.38%), reflecting population loss associated with migration, population aging, and declining fertility rates. These contrasts illustrate distinct stages of the demographic transition, shaped by economic conditions, social structures, and public policy interventions.

Figure 5 highlights significant changes in age structure across all clusters, marked by a contraction at the base of the population pyramid (declining fertility) and an expansion at the top (increasing longevity). BSA I experienced a gradual demographic transition, consistent with its relatively stable climate. BSA II showed a more accelerated narrowing of the base, closely linked to agricultural dynamics, while BSA III exhibited moderate population aging under semi-arid conditions. BSA IV stands out for its advanced aging profile, potentially associated with the outmigration of younger populations. These patterns underscore the strong interaction between climatic conditions and socioeconomic characteristics in shaping regional demographic dynamics.

Between 1991 and 2010, all climate clusters (BSA I, II, III, and IV) exhibited a pronounced decline in the total fertility rate (TFR), accompanied by a consistent increase in life expectancy at birth, reflecting an advanced demographic transition process and overall improvements in living conditions. BSA I experienced the most substantial reduction in TFR, declining from 4.41 to 2.17 children per woman (a decrease of 50.9%), while life expectancy increased markedly from 58.73 to

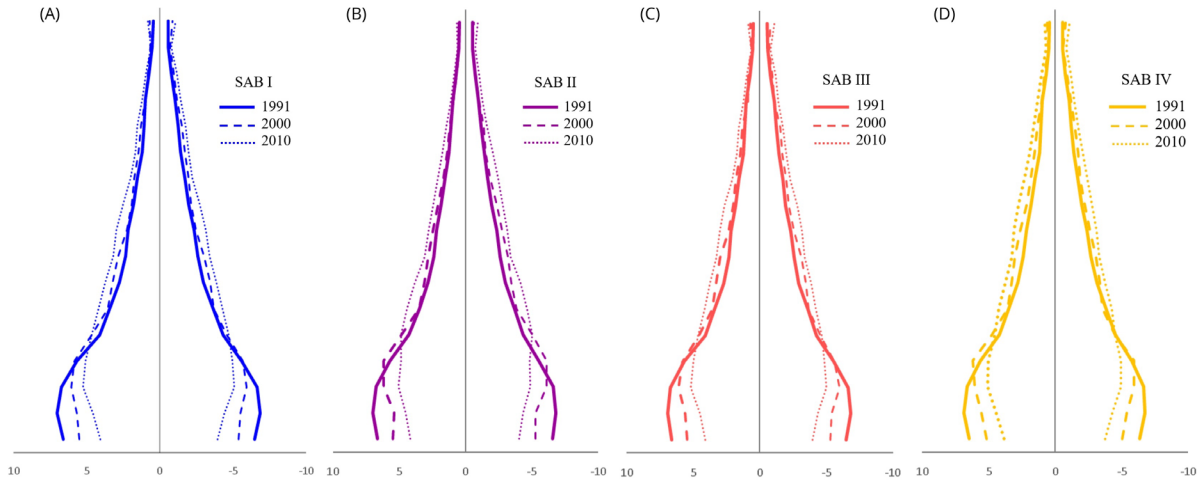

Figure 5 – Age pyramids of climate clusters BSA I, II, III, and IV in the 1991, 2000, and 2010 population censuses.

70.92 years. These trends suggest that improved access to healthcare and education, combined with relatively stable climatic conditions, contributed simultaneously to declining fertility rates and increased longevity. BSA IV recorded the lowest fertility rate among the clusters in 2010 (2.16 children per woman, corresponding to a 47.7% reduction) and the highest life expectancy, which rose from 61.96 to 72.32 years. This pattern indicates that, despite the presence of milder climatic conditions, socioeconomic processes—particularly youth out-migration and population aging—play a decisive role in shaping demographic dynamics within this cluster (Table 2).

Urbanization rates across the BSA climate clusters increased markedly between 1991 and 2010, reflecting the growing concentration of

Table 2 – Distribution of the population by age group and sociodemographic indicators in climate clusters BSA I, II, III, and IV.

Indicator	Census			Variation (%)		
	1991	2000	2010	1991–2000	2000–2010	1991–2010
BSA I						
Total population	**9,620,245**	**10,506,099**	**11,522,689**	**9.2**	**9.7**	**19.8**
% of women	50.89	50.63	50.81	−0.5	0.4	−0.2
Median age	19.26	22.39	26.91	16.3	20.2	39.7
Population under 15 years	40.40	34.08	27.35	−15.66	−19.73	−32.30
Population aged 15–64 years	53.93	59.07	64.56	9.54	9.29	19.72
Population aged 65 years and over	5.67	6.85	8.09	20.85	18.01	42.62
Sex ratio	96.51	97.52	96.83	1.0	−0.7	0.3
Total dependency ratio	86.18	69.78	55.17	−19.0	−20.9	−36.0
Aging index	6.14	6.85	8.07	11.6	17.9	31.6
Life expectancy at birth	58.73	64.86	70.92	10.4	9.3	20.8
Total fertility rate	4.41	3.12	2.17	−29.3	−30.5	−50.9
Infant mortality	75.81	49.37	24.98	−34.9	−49.4	−67.0
Under-five mortality	97.92	60.53	26.65	−38.2	−56.0	−72.8
Illiteracy rate—15 years or older	47.01	33.94	25.17	−27.8	−25.8	−46.5
Proportion of poor population	73.02	58.72	36.62	−19.6	−37.6	−49.9
% of households with piped water	34.53	48.65	75.31	40.9	54.8	118.1

Continues...

Table 2 – Continuation.

Indicator	Census			Variation (%)		
	1991	2000	2010	1991–2000	2000–2010	1991–2010
% of urban households with garbage collection	54.23	79.67	93.35	46.9	17.2	72.1
% of households with electricity	61.19	84.33	98.13	37.8	16.4	60.4
% of households with inadequate water and sanitation	38.25	20.82	17.96	−45.6	−13.7	−53.0
% of urbanization	50.50	57.92	63.13	14.7	9.0	25.0
IDHM	0.327	0.452	0.611	38.3	35.3	87.1
					1991–2000	**2000–2010**
Annual growth rate (%)					0.89	0.93
BSA II						
Total population	**1,914,424**	**2,148,406**	**2,391,194**	**12.2**	**11.3**	**24.9**
% of women	51.42	51.20	51.43	−0.4	0.4	0.0
Median age	19.30	22.01	26.86	14.0	22.0	39.2
Population under 15 years	40.33	33.72	27.06	−16.37	−19.77	−32.91
Population aged 15–64 years	54.32	60.68	65.77	11.69	8.40	21.08
Population aged 65 years and over	5.35	5.60	7.17	4.67	28.03	34.01
Sex ratio	94.49	95.30	94.46	0.9	−0.9	0.0
Total dependency ratio	85.00	65.53	52.66	−22.9	−19.6	−38.0
Aging index	4.51	5.60	7.15	24.1	27.6	58.4
Life expectancy at birth	61.85	65.76	71.83	6.3	9.2	16.1
Total fertility rate	4.00	2.89	2.03	−27.8	−29.8	−49.4
Infant mortality	61.00	41.52	23.08	−31.9	−44.4	−62.2
Under-five mortality	79.83	53.62	25.03	−32.8	−53.3	−68.7
Illiteracy rate — 15 years or older	40.60	29.35	21.78	−27.7	−25.8	−46.4
Proportion of poor population	70.07	55.75	32.04	−20.4	−42.5	−54.3
% of households with piped water	35.78	49.41	86.68	38.1	75.4	142.3
% of urban households with garbage collection	30.79	57.64	81.03	87.2	40.6	163.2
% of households with electricity	61.09	80.76	96.50	32.2	19.5	57.9
% of households with inadequate water and sanitation	32.51	8.94	7.37	−72.5	−17.6	−77.3
% of urbanization	61.63	69.58	71.30	12.9	2.5	15.7
IDHM	0.368	0.486	0.649	32.3	33.5	76.6
					1991–2000	**2000–2010**
Annual growth rate (%)					1.17	1.08
BSA III						
Total population	**6.929.150**	**7.586.043**	**8.323.236**	**9.5**	**9.7**	**20.1**
% of women	50.90	50.53	50.60	−0.7	0.1	−0.6
Median age	19.34	22.59	27.25	16.8	20.6	40.9
Population under 15 years	40.22	33.85	27.05	−15.83	−20.09	−32.74
Population aged 15–64 years	53.93	59.52	64.79	10.36	8.85	20.13
Population aged 65 years and over	5.85	6.63	8.16	13.3	23.13	39.51
Sex ratio	96.45	97.91	97.64	1.5	−0.3	1.2
Total dependency ratio	84.80	68.44	54.61	−19.3	−20.2	−35.6

Continues...

Table 2 – Continuation.

Indicator	Census			Variation (%)		
	1991	2000	2010	1991–2000	2000–2010	1991–2010
Aging index	5.78	6.63	8.12	14.7	22.5	40.5
Life expectancy at birth	60.27	66.17	71.38	9.8	7.9	18.4
Total fertility rate	4.16	2.99	2.23	−28.1	−25.4	−46.4
Infant mortality	68.09	44.77	23.34	−34.2	−47.9	−65.7
Under-five mortality	88.65	56.46	25.01	−36.3	−55.7	−71.8
Illiteracy rate—15 years or older	45.70	33.05	24.60	−27.7	−25.6	−46.2
Proportion of poor population	75.66	58.81	36.12	−22.3	−38.6	−52.3
% of households with piped water	33.38	50.45	77.79	51.2	54.2	133.1
% of urban households with garbage collection	46.50	73.29	92.39	57.6	26.1	98.7
% of households with electricity	56.58	81.10	96.79	43.3	19.3	71.1
% of households with inadequate water and sanitation	45.79	13.40	11.03	−70.7	−17.7	−75.9
% of urbanization	49.36	57.18	62.11	15.8	8.6	25.8
IDHM	0.331	0.465	0.626	40.5	34.6	89.2
					1991–2000	**2000–2010**
Annual growth rate (%)					0.92	0.93
BSA IV						
Total population	**6.356.232**	**6.677.022**	**6.935.761**	**5.0**	**3.9**	**9.1**
% of women	50.12	49.94	50.16	−0.4	0.4	0.1
Median age	19.54	22.59	27.76	15.6	22.9	42.1
Population under 15 years	39.69	33.13	26.31	−16.53	−20.57	−33.7
Population aged 15–64 years	54.85	60.56	65.38	10.41	7.96	19.20
Population aged 65 years and over	5.46	6.31	8.31	15.58	31.59	52.08
Sex ratio	99.50	100.23	99.37	0.7	−0.9	−0.1
Total dependency ratio	83.15	69.25	53.20	−16.7	−23.2	−36.0
Aging index	5.07	6.67	8.29	31.5	24.3	63.5
Life expectancy at birth	61.96	65.84	72.32	6.3	9.9	16.7
Total fertility rate	4.12	3.16	2.16	−23.4	−31.7	−47.7
Infant mortality	56.74	40.54	21.26	−28.5	−47.6	−62.5
Under-five mortality	72.88	48.71	23.39	−33.2	−52.0	−67.9
Illiteracy rate—15 years or older	39.19	29.57	19.59	−24.5	−33.8	−50.0
Proportion of poor population	70.73	59.84	31.22	−15.4	−47.8	−55.9
% of households with piped water	37.98	46.84	81.56	23.3	74.1	114.8
% of urban households with garbage collection	45.73	69.93	93.34	52.9	33.5	104.1
% of households with electricity	57.89	73.41	96.22	26.8	31.1	66.2
% of households with inadequate water and sanitation	25.09	18.02	9.58	−28.2	−46.8	−61.8
% of urbanization	48.35	47.71	62.86	−1.3	31.7	30.0
IDHM	0.336	0.447	0.635	33.3	41.9	89.1
					1991–2000	**2000–2010**
Annual growth rate (%)					0.50	0.38

Source: prepared by the authors based on data from the Brazilian Institute of Geography and Statistics (IBGE) (1991, 2000, and 2010).

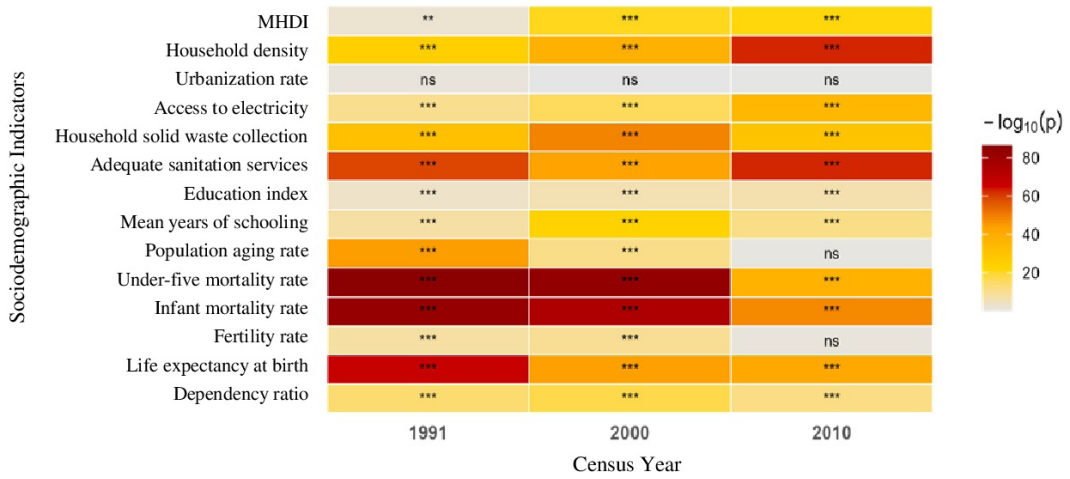

Figure 6 – Heatmap of global significance (–$\log_{10}$ p) by variable and census year for sociodemographic indicators.
Note: Colors represent the magnitude of statistical significance, expressed as –$\log_{10}$(p), obtained from Kruskal–Wallis tests applied to the four spatial climate clusters of the Brazilian Semi-Arid Region (BSA). Asterisks denote significance levels as follows: ns (p≥0.05), *(p<0.05), **(p<0.01), ***(p<0.001).

the population in urban areas, driven by a combination of socioeconomic processes and regional climatic characteristics. In 2010, BSA II stood out for exhibiting the most pronounced growth, increasing from 61.63 to 71.30%, highlighting the combined role of favorable climatic conditions and economic dynamics in shaping urbanization patterns.

Regarding illiteracy rates, all clusters exhibited substantial declines over the study period, with BSA IV showing the largest proportional reduction (55.9%), decreasing from 70.73 to 31.22%. This cluster is characterized by milder climatic conditions and moderate humidity, which may be associated with improved living conditions and enhanced access to education and public services, although socioeconomic and institutional factors remain decisive in explaining these advances.

Between 1991 and 2010, the BSA recorded significant advances in basic sanitation and infrastructure services, including expanded access to piped water, solid waste collection, and electricity across all clusters, changes partly shaped by regional climatic conditions and public investment strategies (Rodrigues et al., 2022).

Over the same period, the MHDI in the BSA increased substantially, indicating overall improvements in population living conditions, despite persistent challenges associated with climatic variability. BSA II, characterized by higher precipitation and elevated temperatures, exhibited the largest increase in MHDI, rising from 0.368 to 0.649, suggesting a relative balance between favorable environmental conditions and socioeconomic progress.

Overall, the results indicate significant advances in human development across all four BSA clusters, with MHDI values reaching the medium development category. According to Santos et al. (2015), these improvements reflect the effects of relatively successful public policies, although continued and targeted efforts remain necessary to achieve high or very high MHDI levels across the region.

The preceding descriptive analyses revealed marked contrasts among the climate clusters, which were statistically confirmed by the global Kruskal-Wallis test (Figure 6). Most variables displayed statistically significant differences between groups, with the exception of the urbanization rate and a limited number of variables in 2010, such as the fertility rate and population aging rate. These findings indicate consistent associations between climatic context and demographic, educational, and infrastructure indicators, suggesting that environmental conditions may indirectly influence regional human development, while not implying direct causal relationships.

Discussion

The BSA faces climatic challenges such as irregular rainfall and aridity, which intensify socioeconomic and environmental vulnerabilities and are closely associated with economic stagnation and persistent poverty (Buriti and Barbosa, 2022; Oliveira et al., 2024). Nevertheless, poverty in the region cannot be attributed solely to climatic factors, as it is also the result of historical processes of land concentration and political power that have perpetuated structural inequalities over time (Buriti et al., 2020; Gomes and Zanella, 2023).

The BSA comprises subregions with distinct characteristics. BSA I exhibits notable social advances but remains vulnerable to recurrent droughts; BSA II shows strong population growth associated with agricultural activities, yet is increasingly affected by declining rainfall; BSA III faces demographic constraints but has achieved improvements in human development indicators; and BSA IV is characterized by population decline and advanced aging. Climatic conditions directly affect agricultural dynamics across these subregions. While the economic growth of BSA II may be constrained by decreasing precipitation, BSA III experiences agricultural limitations that accelerate rural outmigra-

tion, and BSA IV, despite relatively favorable climatic conditions, faces demographic challenges driven primarily by socioeconomic factors (Moura et al., 2019; Ferreira et al., 2023).

Population dynamics in the BSA are characterized by demographic growth and urbanization levels below the national average of 87.4%, according to IBGE data (2022) and are strongly influenced by the specific climatic conditions of each subregion. BSA I, benefiting from greater climatic stability, exhibits accelerated population growth and urban expansion but continues to face challenges such as land concentration and limited economic opportunities. BSA II records the highest rates of population growth and urbanization, largely driven by agricultural expansion. In contrast, BSA III, despite pronounced climatic adversities, demonstrates relative resilience, reflected in improvements in human development indicators. BSA IV presents the lowest population growth rates and a more advanced aging structure, reflecting persistent constraints on local socioeconomic opportunities (Costa and Ojima, 2020).

Climate change has progressively intensified the challenges faced by arid and semi-arid regions such as the BSA, posing increasing risks to water availability for agriculture and directly affecting agricultural production and food security in local communities. Additionally, climate change contributes to ecosystem degradation and accelerates biodiversity loss, thereby threatening the sustainability of family farming systems. These systems depend directly on natural resources and climatic conditions to sustain livelihoods and support regional socioeconomic development (Ortiz et al., 2022; Lemos and Bezerra, 2023).

The analysis of the BSA reveals a demographic transition marked by declining fertility rates, increased life expectancy, and population aging, albeit with pronounced inequalities among subregions. BSA I and BSA II show socioeconomic progress but increasingly face challenges related to population aging and growing pressure on health services. In contrast, BSA III and BSA IV, characterized by more severe climatic constraints, experience significant youth outmigration, accelerated population aging, and persistent deficits in economic and social opportunities. These dynamics constitute a substantial barrier to achieving sustainable economic and social development in these subregions (Dias et al., 2023; Costa and Ojima, 2024).

Conclusion

The results of this research demonstrate the high vulnerability of the BSA to climate change, which is intensified by the interaction between environmental and socioeconomic factors. The integrated analysis of meteorological data and social indicators identified a significant increase in both the frequency and intensity of extreme climate events, including prolonged droughts, rising mean temperatures, and the expansion of arid conditions. These processes directly affect water availability, biodiversity, and productive activities, particularly subsistence agriculture and livestock farming.

The development of a homoclimatic typology for the BSA proved to be a key methodological contribution, as it enabled a more comprehensive understanding of the region's internal climatic diversity and atmospheric dynamics. The findings confirm the marked climatic heterogeneity of the BSA and reinforce the relevance of multivariate regional analyses. BSA I, characterized by higher humidity levels and moderate temperatures, exhibits lower vulnerability, whereas BSA III, defined by more arid conditions and greater water deficits, shows increased susceptibility to desertification.

From a sociodemographic perspective, the results indicate a trend toward population aging, declining fertility and mortality rates, and gradual improvements in basic infrastructure as well as education and sanitation indicators. These patterns suggest a relative improvement in living conditions, although pronounced intra-regional inequalities and persistent structural vulnerabilities remain. The integration of climatic and social data strengthens the argument that vulnerability in the BSA cannot be explained solely by natural conditions, but is also shaped by historical inequalities and institutional limitations. Accordingly, the findings underscore the need for integrated public policies with explicit territorial and climatic perspectives, focused on sustainable water resource management, the promotion of adaptive technologies, and the strengthening of social and institutional infrastructure.

In summary, this study highlights the importance of jointly analyzing demographic and climatic dynamics in the BSA region. Future research may benefit from the application of more advanced statistical approaches and spatial analysis techniques, with greater temporal depth and the inclusion of additional environmental and socioeconomic variables. Such efforts can refine climate regionalization and deepen the understanding of climate–society interactions, thereby supporting the formulation of more adaptive, equitable, and effective public policies for the region.

Authors' Contributions

Machado, R.B.M.: conceptualization; data curation; formal analysis; investigation; methodology; writing — original draft; writing — review & editing. **Batista**, F.F.: formal analysis; investigation; methodology; writing — review & editing. **Andrade**, L.M.B.: methodology; supervision; writing — review & editing. **Silva**, C.M.S.: methodology; supervision; writing — review & editing. **Martins**, A.S.F.S.: investigation; methodology.

References

Abreu, L.; Mutti, P.; Lima, K., 2019. Variabilidade espacial e temporal da precipitação na bacia hidrográfica do Rio Parnaíba, Nordeste do Brasil. Revista Brasileira de Meio Ambiente, v.7 (2), 82-97. https://doi.org/10.5281/zenodo.3524759.

Albuquerque, Y.R.T.; Almeida, A.Q.; Arcieri, M.S.; Mendes, L.A., 2020. Definição de regiões hidrologicamente homogêneas a partir de técnicas de estatística multivariada na bacia hidrográfica do Rio Itapicuru - BA com base em dados físico-climáticos e de sensoriamento remoto. Caminhos de Geografia, v. 21 (78), 290-302. https://doi.org/10.14393/RCG217853077.

Alvar-Beltrán, J.; Gobin, A.; Orlandini, S.; Dao, A.; Marta, A.D., 2021. Climate resilience of irrigated quinoa in semi-arid West Africa. Climate Research, v. 84, 97-111. https://www.jstor.org/stable/27120977.

Alves, L.; Gomes, H.; Correia Filho, W.; Oliveira Júnior, J.; Gonçalves, L.; Herdies, D.; Silva, F., 2021. Identificação das regiões pluviométricas homogêneas e início e fim da estação chuvosa na bacia do médio São Francisco (Brasil). Caminhos de Geografia, v. 22 (80), 267-281. https://doi.org/10.14393/RCG228055013.

Barbosa, H.A., 2023. Flash Drought and Its Characteristics in Northeastern South America during 2004–2022 Using Satellite-Based Products. Atmosphere, v. 14 (11), 1629. https://doi.org/10.3390/atmos14111629.

Barbosa, H.A., 2024. Understanding the rapid increase in drought stress and its connections with climate desertification since the early 1990s over the Brazilian semi-arid region, Journal of Arid Environments, v. 222. https://doi.org/10.1016/j.jaridenv.2024.105142.

Blanco, P.S.; Doyle, M.E., 2024. Temporal variability of aridity in Argentina during the period 1961–2020, Atmospheric Research, v. 310. https://doi.org/10.1016/j.atmosres.2024.107613.

Brito, C.S.; Silva, R.M.; Santos, C.A.G.; Brasil Neto, R.M.; Coelho, V.H.R., 2021. Monitoring meteorological drought in a semiarid region using two long-term satellite-estimated rainfall datasets: a case study of the Piranhas River basin, northeastern Brazil, Atmospheric Research, v. 250, 105380. https://doi.org/10.1016/j.atmosres.2020.105380.

Buriti, C.O.; Barbosa, H.A., 2022. Desertificação e mapeamento de áreas degradadas no Semiárido brasileiro a partir de satélites In: Magnoni Junior, L. (orgs.), Ensino de geografia e a redução do risco de desastres em espaços urbanos e rurais. CPS, São Paulo, pp. 465-483. https://doi.org/10.57243/BHUG1272.

Burrell, A.L; Evans, J.P.; De Kauwe, M.G., 2020. Anthropogenic climate change has driven over 5 million km2 of drylands towards desertification. Nature Communications, v. 1, 3853. https://doi.org/10.1038/s41467-020-17710-7.

Costa, P.V.M.; Ojima, R., 2020. Transposição do rio São Francisco e a vulnerabilidade sociodemográfica: desafios ao bem-estar da população sertaneja. Desenvolvimento e Meio Ambiente, v. 55. https://doi.org/10.5380/dma.v55i0.73381.

Dias, E.M.S.; Pessoa, Z.S.; Teixeira, R.L.P., 2023. Governança adaptativa e segurança hídrica em contexto de mudanças climáticas no semiárido, Mercator, v. 21, 1-11. https://doi.org/10.4215/rm2022.e21025.

Dzvene, A.R; Zhou, L.; Slayi, M.; Dirwai, T.L., 2025. A scoping review on challenges and measures for climate change in arid and semi-arid agri-food systems. Discover Sustainability, v. 6 (151). https://doi.org/10.1007/s43621-025-00945-z.

Espinoza, J-C.; Jimenez, J C.; Marengo, J A.; Schongart, J.; Ronchail, J.; Lavado-Casimiro, W., 2024. The new record of drought and warmth in the Amazon in 2023 related to regional and global climatic features. Scientific Reports, v. 14, 8107. https://doi.org/10.1038/s41598-024-58782-5.

Everitt, B.; Dunn, G., 2010. Applied multivariate analysis. Arnold, London, 2. ed., 354 p.

Everitt, B.; Landau, S.; Leese, M., 2011. *Cluster* analysis. Arnold, London, 5. ed., 330 p.

Ferreira, J.G.; Gomes, M.F.B.; Figueredo, E.S.; Xavier, J.S., 2023. Água, semiárido e sustentabilidade: aplicando o ODS 6 aos municípios do Rio Grande do Norte. IX Sustentável, v. 9 (2), 75-90.

Gomes, F.I.B.P.; Zanella, M.E., 2023. Histórico, causas e características da semiaridez do Nordeste do Brasil. Geografares, v. 3 (37). https://doi.org/10.47456/geo.v3i37.41515.

Guedes, G.; Noronha, K.; Andrade, L.; Rodrigues, D.; Martins, A., 2024. Un enfoque secuencial y espacial a las precipitaciones extremas y las condiciones sociodemográficas relacionadas con los desastres naturales en la región semiárida del Brasil. Notas de Población (Impresa), v. 51 (118), 111-148 (Accessed January, 22, 2024) at:. https://hdl.handle.net/11362/80541.

Hair, J.; Black, W.; Babin, B., 2009. Análise multivariada de dados. Bookman, Porto Alegre, 6. ed., 682 p.

Huang, J., 2020. Global desertification vulnerability to climate change and human activities. Land Degradation & Development, v. 31 (11), 1380-1391. https://doi.org/10.1002/ldr.3556.

Huang, J.; Ji, M.; Xie, Y.; Wang, S.; He, Y.; Ran, J., 2016. Global semi-arid climate change over last 60 years. Climate Dynamics, v. 46 (3), 1131-1150. https://doi.org/10.1007/s00382-015-2636-8.

Instituto Brasileiro de Geografia e Estatística (IBGE), 1991. Censo Brasileiro de 1991. IBGE, Rio de Janeiro.

Instituto Brasileiro de Geografia e Estatística (IBGE), 2000. Censo Brasileiro de 2000. IBGE, Rio de Janeiro.

Instituto Brasileiro de Geografia e Estatística (IBGE), 2010. Censo Brasileiro de 2010. IBGE, Rio de Janeiro.

Instituto Brasileiro de Geografia e Estatística (IBGE), 2022. Censo Brasileiro de 2021. IBGE, Rio de Janeiro.

IPCC, 2023: Climate Change 2023: Synthesis Report. Contribution of Working Groups I, II and III to the Sixth Assessment Report of the Intergovernmental Panel on Climate Change [Core Writing Team, H. Lee and J. Romero (eds.)]. IPCC, Geneva, Switzerland, pp. 35-115. https://doi.org/10.59327/IPCC/AR6-9789291691647.

Lattin, J.; Carroll, J.; Green, P., 2011, Análise de dados multivariados. Cengage Learning, São Paulo, 475 p.

Lemos, J.J.S.; Bezerra, F.N.R., 2023. Climate Resilience Agriculture (CRA) In The Brazilian Semi-Arid Region. IOSR Journal Of Humanities And Social Science, v. 28 (8). https://doi.org/10.9790/0837-2808080110.

Marengo, J., 2024. Impactos sociais dos eventos climáticos extremos. Ciência e Cultura, v. 76, 1-8. https://doi.org/10.5935/2317-6660.20240068.

Marengo, J.; Torres, R.; Alves, L., 2017. Drought in Northeast Brazil - past, present, and future. Theoretical and Applied Climatology, v. 129 (3), 1189-1200. https://doi.org/10.1007/s00704-016-1840-8.

Marengo, J.A.; Cunha, A.P.M.A.; Nobre, C.A.; Neto, G.G.R.; Magalhaes, A.R.; Torres, R.R.; Sampaio, G.; Alexandre, F.; Alves, L.M.; Cuartas, L.A.; Deusdará, K.R.L.; Álvala, R.C.S., 2020. Assessing Drought in the Drylands of Northeast Brazil under Regional Warming Exceeding 4 °C. Natural Hazards, v. 103, 2589-2611. https://doi.org/10.1007/s11069-020-04097-3.

Medeiros, F.; Oliveira, C.; Torres, R., 2020. Climatic aspects and vertical structure circulation associated with the severe drought in Northeast Brazil (2012–2016). Climate Dynamics, v. 55, 2327-2341. https://doi.org/10.1007/s00382-020-05385-1.

Mingoti, S., 2013. Análise de dados através de métodos de estatística multivariada: uma abordagem aplicada. Editora UFMG, Belo Horizonte, 297 p.

Moura, M. de; Sobrinho, J.; Silva, T., 2019. Aspectos meteorológicos do semiárido brasileiro. In: Ximenes, L.; Silva, M.; Brito, L. (orgs.), Tecnologias de convivência com o semiárido brasileiro. Banco do Nordeste do Brasil, Fortaleza, pp. 85-104.

Mutti, P.R.; Abreu, L.P.; Andrade, L.M.B.; Spyrides, M.H.C.; Lima, K.C.; Oliveira, C.P; Dubreuil, V.; Bezerra, B.G., 2020. A detailed framework for the characterization of rainfall climatology in semiarid watersheds. Theoretical and Applied Climatology, v. 139, 109-125. https://doi.org/10.1007/S00704-019-02963-0.

Nobre, C.; Marengo, J.; Seluchi, M.; Cuartas, L.; Alves, L., 2016. Some Characteristics and Impacts of the Drought and Water Crisis in Southeastern Brazil during 2014 and 2015. Journal of Water Resource and Protection, v. 8(2), 252-262. https://doi.org/10.4236/jwarp.2016.82022.

Oliveira, P.; Silva, C.; Lima, K., 2016. Climatology and trend analysis of extreme precipitation in subregions of Northeast Brazil. Theoretical and Applied Climatology, v. 130, 77-90. https://doi.org/10.1007/s00704-016-1865-z.

Oliveira, V.L.C.; Carvalho, J.N.; Cestaro, L.A.; Souza, J.J.L.L., 2024. Soil erosion vulnerability in Brazilian semiarid. Revista Brasileira de Geomorfologia, v. 25 (2). https://doi.org/10.20502/rbg.v24i2.2451.

Ortiz, A.C.; Jin, L.; Ogrinc, N.; Kaye, J.; Krajnc, B.; Ma, L., 2022. Dryland irrigation increases accumulation rates of pedogenic carbonate and releases soil abiotic CO_2. Scientific Reports, v. 12, 464. https://doi.org/10.1038/s41598-021-04226-3.

Paredes-Trejo, F.; Barbosa, H.A.; Daldegan, G.A.; Teich, I.; García, C.L.; Kumar, T.V.L.; Buriti, C.O., 2023. Impact of drought on land productivity and degradation in the Brazilian Semiarid Region. Land, v. 12 (5), 954. https://doi.org/10.3390/land12050954.

R Core Team, 2023. R: A Language and Environment for Statistical Computing_. R Foundation for Statistical Computing, Vienna, Austria (Accessed January, 22, 2024) at:. https://www.R-project.org/.

Rathore, P., 2024. Climate change adaptation and resource resilience in Semi-Arid Regions: strategies, challenges, and case studies. Journal for Research in Applied Sciences and Biotechnology, v. 3, 119-130. https://doi.org/10.55544/jrasb.3.5.14.

Reis, L.; Santos, C.; Bezerra, B.; Mutti, P.; Spyrides, M.; Silva, P.; Magalhães, T.; Ferreira, R.; Rodrigues, D.; Andrade, L., 2020. Influence of Climate Variability on Soybean Yield in MATOPIBA, Brazil. Atmosphere, v. 11, 1130. https://doi.org/10.3390/atmos11101130.

Reis, L.C.; Silva, C.M.S.; Bezerra, B.G.; Mutti, P.R.; Spyrides, M.H.C.; Silva, P.E., 2020. Analysis of Climate Extreme Indices in the MATOPIBA Region, Brazil. Pure and Applied Geophysics, v. 177, 4457-4478. https://doi.org/10.1007/s00024-020-02474-4.

Ribeiro, M.; Andrade, L.; Spyrides, M.; Silva, P., 2022. Sanitary, social, and meteorological aspects and natural disasters in the Northeastern Region of Brazil. Mercator, v. 21, 1984-2201. https://doi.org/10.4215/rm2022.e21009.

Rodrigues, E.; Coutinho, A.; Souza, J.; Costa, I.; Santos Neto, S.; Antonino, A., 2022. Rural Sanitation: scenarios and public policies for the brazilian semi-arid region. Sustainability, v. 14 (12), 7157. https://doi.org/10.3390/su14127157.

Santana, A.; Santos, R., 2020. Impactos da seca de 2012-2017 na Região Semiárida do Nordeste: notas sobre a abordagem de dados quantitativos e conclusões qualitativas. Boletim Regional, Urbano e Ambiental, v. 22, 119-129. https://doi.org/10.38116/brua22art9.

Santos, A.; Gonçalves, W.; Andrade, L.; Rodrigues, D.; Batista, F.; Lima, G.; Silva, C., 2024. Space–Time Characterization of Extreme Precipitation Indices for the Semiarid Region of Brazil. Climate, v. 12(3), 43. https://doi.org/10.3390/cli12030043.

Santos, A.; Gonçalves, W.; Rodrigues, D.; Andrade, L.; e Silva, C., 2022. Evaluation of Extreme Precipitation Indices in Brazil's Semiarid Region from Satellite Data. Atmosphere, v. 13 (10), 1598. https://doi.org/10.3390/atmos13101598.

Santos, H.; Silva, J.; Portugal, J., 2015. Análise espacial do índice de desenvolvimento humano municipal na região semiárida brasileira. Revista Brasileira de Geomática, v. 3 (2), 70-76. https://doi.org/10.3895/rbgeo.v3n2.5475.

Sanzheev, E.D.; Mikheeva, A.S.; Osodoev, P.V.; Batomunkuev, V.S.; Tulokhonov, A.K., 2020. Theoretical approaches and practical assessment of socio-economic effects of desertification in Mongolia. International Journal of Environmental Research and Public Health, v. 17(11), 4068. https://doi.org/10.3390/ijerph17114068.

Scholes, R.J., 2020. Zhe Future of Semi-Arid Regions: A Weak Fabric Unravels. The Climate, v. 8 (3), 43. https://doi.org/10.3390/cli8030043.

Silva, L.; Souza, C.; Silva, C.R.; Filgueiras, R.; Sena-Souza, J.; Fernandes Filho, E.; Leite, M., 2023. Mapping the effects of climate change on reference evapotranspiration in future scenarios in the Brazilian Semiarid Region - South America. Revista Brasileira de Geografia Física, v. 16 (2), 1001-1012. https://doi.org/10.26848/rbgf.v16.2.p1001-1012.

Silveira, K.; Andrade, L.; Spyrides, M.; e Silva, C..; de Oliveira, C.; Guedes, B.; Mutti, P., 2020. Climate Profiles in Brazilian Microregions. Atmosphere, v. 11, 1217. https://doi.org/10.3390/atmos11111217.

Souza, L.; Moura, M. de; Sediyama, G.; Silva, T., 2015. Balanço de energia e controle biofísico da evapotranspiração na Caatinga em condições de seca intensa. Pesquisa Agropecuária Brasileira, v. 50 (8). https://doi.org/10.1590/S0100-204X2015000800001.

Superintendência do Desenvolvimento do Nordeste (SUDENE), 2021. Relatório Final Preliminar para delimitação do Semiárido. Ministério do Desenvolvimento Regional, 272 p.

Tinôco, I.; Bezerra, B.; Lucio, P.; Barbosa, L, 2018. Characterization of rainfall patterns in the semiarid Brazil. Anuário do Instituto de Geociências, v. 41, 397-409. https://doi.org/10.11137/2018_2_397_409.

Tomasella, J.; Vieira, R.M.S.P.; Barbosa, A.A.; Rodriguez, D.A.; Santana, M.O.; Sestini, M.F., 2018. Desertifcation trends in the Northeast of Brazil over the period 2000–2016. International Journal of Applied Earth Observation and Geoinformation, v. 73, 197-206. https://doi.org/10.1016/j.jag.2018.06.012.

Ullah, W.; Wang, G.; Lou, D.; Ullah, S.; Bhatti, A.S.; Ullah, S.; Karim, A.; Hagan, D.F.T.; Ali, G., 2021. Large-scale atmospheric circulation patterns associated with extreme monsoon precipitation in Pakistan during 1981–2018, Atmospheric Research, v. 253, 105489. https://doi.org/10.1016/j.atmosres.2021.105489.

Vaidyanathan, A.; Malilay J.; Schramm, P.; Saha, S., 2020. Heat-Related Deaths — United States, 2004–2018. Morbidity and Mortality Weekly Report, v. 69 (24), 729-734. https://doi.org/10.15585/mmwr.mm6924a1.

Vieira, R.M.D.S.P; Tomasella, J.; Barbosa, A.A.; Martins, M.A.; Rodriguez, D.A.; Rezende, F. S.; Santana, M. D. Desertification risk assessment in Northeast Brazil: Current trends and future scenarios. Land Degradation & Development, v. 32 (1), 224-240. https://doi.org/10.1002/ldr.3681.

Ward, J., 1963. Hierarchical grouping to optimize an objective function. Journal of the American Statistical Association, v. 58, 236-244.

Wilks, D.S., 2011. Statistical Methods in the Atmospheric Sciencies_2011. International Geophycs Series, p. 649.

Xavier, A.; Scanlon, B.; King, C.; Alves, A., 2022. New improved Brazilian daily weather gridded data (1961–2020). International Journal of Climatology, v. 42 (16), 8390-8404. https://doi.org/10.1002/joc.7731.

Yao, J.; Liu, H., Huang, J.; Gao, Z.; Wang, G.; Li, D.; Yu, H.; Chen, X., 2020. Accelerated dryland expansion regulates future variability in dryland gross primary production. Nature Communications, v. 11, 1665. https://doi.org/10.1038/s41467-020-15515-2.

Zabalaga, D.; da Rocha, R.; LLopart, M.; Reboita, M., 2022. Identificação de Regiões Homogêneas de Precipitação e Projeções Climáticas com o RegCM4 no Altiplano Andino. Revista Brasileira de Geografia Física, v. 15 (6), 2689-2703. https://doi.org/10.26848/rbgf.v15.6.p2689-2703.